Journal of Pharmaceutical and Biomedical Analysis 54 (2011) 503–509

Contents lists available at ScienceDirect

Journal of Pharmaceutical and Biomedical Analysis

journal homepage: www.elsevier.com/locate/jpba

Effect of cyclodextrins on the solubility and stability of candesartan cilexetil in solution and solid state

Alaa' A. Al Omari [a], Mahmoud M. Al Omari [b], Adnan A. Badwan [b], Khaldoun A. Al-Sou'od [a,*]

[a] Department of Chemistry, Al al-Bayt University, Mafraq, Jordan
[b] The Jordanian Pharmaceutical Manufacturing Company, Naor, Jordan

ARTICLE INFO

Article history:
Received 20 May 2010
Received in revised form 30 August 2010
Accepted 19 September 2010
Available online 29 September 2010

Keywords:
Candesartan cilexetil
Cyclodextrin
Solubility
Stability
Molecular modelling

ABSTRACT

Guest–host interactions of candesartan cilexetil (CAND) with cyclodextrins (CyDs) have been investigated using phase solubility diagrams (PSD), X-ray powder diffractometry (XRPD), differential scanning calorimetry (DSC) and molecular mechanical modelling (MM). Estimates of the complex formation constant (K_{11}) show that the tendency of CAND ($pK_a = 6.0$) to complex with CyDs follows the order: β-CyD > HP-β-CyD > γ-CyD > α-CyD. Complex formation of CAND with β-CyD ($\Delta G^\circ = -31.5$ kJ/mol) is largely driven by enthalpy change ($\Delta H^\circ = -32.8$ kJ/mol) and slightly retarded by entropy change ($\Delta S^\circ = -4.6$ J/mol K). The HPLC results indicate that complex prepared by freeze drying method is chemically not stable due to the formation of amorphous CAND. Also it may suggest formulating CAND with β-CyD by kneading (dispersion) or co-evaporation (real inclusion complex) methods into capsule rather than compressed in tablets, where the compression enhances the instability of CAND. DSC thermograms for CAND/β-CyD complexes proved the formation of inclusion complexes with new solid phase. MM studies indicate the partial penetration of CAND into the β-CyD cavity.

1. Introduction

The use of cyclodextrins (CyDs) in the pharmaceutical industry has grown to a great deal, where different approved pharmaceutical products are already marketed in Japan, the European countries and the USA [1]. The parent CyDs (α-, β-, and γ-CyD) and their derivatives are widely used to improve the solubility of water insoluble compounds through inclusion complexation. Also they are used to enhance the thermal stability, to reduce volatility, and to resist oxidation, hydrolysis and degradation of compounds in solution [2–4].

The antihypertensive drug candesartan cilexetil (CAND) is 2-ethoxy-3-[21-(1*H*-tetrazol-5-yl)biphenyl-4-yl-methyl]-3*H*-benzoimidazole-4-carboxylic acid 1-cyclohexyloxy carbonyloxy-ethyl ester (Fig. 1). In the gastrointestinal tract CAND is converted to candesartan, an angiotensin receptor blocker which blocks the ability of angiotensin II to raise blood pressure by constricting or squeezing arteries and veins, and so leads to a reduction in blood pressure. In addition, by reducing the pressure against which the heart must pump blood, it reduces the work of the heart and is useful in patients with heart failure [5]. It is a white to off-white powder. The solubility in benzyl alcohol is 0.3 M, and the solubility in water is $<8 \times 10^{-8}$ M. The partition coefficient ($C_{octanol}/C_{aqueous}$) at pHs 1.1, 6.9 and 8.9 is >1000 indicating high hydrophobicity character [6]. It has a pK_a value of 6.0 [7].

CAND is stable against temperature, moisture and light in its solid state. When it is formulated into tablet dosage form with excipients it decomposes with the lapse of time due to deformation of crystals caused by molding under elevated pressure in the course of tablet compression [8]. In this study, polyethylene glycol (PEG) was used as an elastic material to improve the stability of CAND in the presence of formulation excipients.

Different types of CAND related compounds were reported and identified in the literature [5,9–11]. CAND undergoes base catalysed hydrolysis and transesterification to form candesartan (cilexetil group was removed from position 22 (Fig. 1)) and methyl and hydroxyethyl candesartans (cilexetil group replaced by methyl and hydroxylethyl groups) [5]. Stenhoff et al. have determined candesartan and desethyl candesartan in human body fluids by HPLC [9]. Desethyl candesartan was formed by removal of the ethyl group from position 15 in addition to cilexetil group). Subba Rao et al. [10] and Mohan et al. [11] have determined and identified several impurities when CAND tablets were subjected to stress conditions of heat and humidity (60 °C and 40 °C/RH 75%). The percentage of these impurities is ranging from 0.05% to 1.25% as measured by HPLC. The impurities include candesartan, methyl and ethyl candesartan, desethyl CAND, 1N-ethyl CAND, 2N-ethyl CAND, 1N-ethyl

* Corresponding author at: P.O. Box 130040, Mafraq 25113, Jordan. Tel.: +962 79 5861350; fax: +962 2 6297025.
E-mail address: khaldoun@aabu.edu.jo (K.A. Al-Sou'od).

0731-7085/$ – see front matter © 2010 Elsevier B.V. All rights reserved.
doi:10.1016/j.jpba.2010.09.027

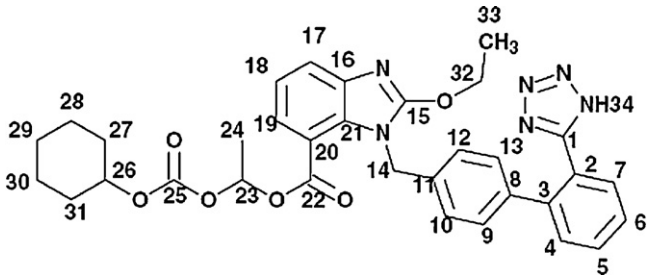

Fig. 1. Molecular structure of candesartan cilexetil.

oxo CAND, 2N-ethyl oxo CAND. The two latter impurities are the desethyl form of the impurities 1N-ethyl CAND, 2N-ethyl CAND.

Interaction of various sartans with CyDs was investigated in solution and in solid state [12–16]. For example, hydroxypropyl-β-cyclodextrin (HP-β-CyD) and methyl-β-cyclodextrin (M-β-CyD) were found to improve the solubility of valsartan [12,13]. The estimated complex formation constants (K_{11}) of the inclusion complexes in un-buffered water were 2.9×10^2 and $5.4 \times 10^2\ M^{-1}$, respectively. Freeze-dried valsartan/HP-β-CyD and co-evaporated valsartan/M-β-CyD (1:1 molar ratio) solid systems offer rapid dissolution profiles in comparison with the profiles of valsartan and its physical mixture with CyD. The thermal stability of solid valsartan at 80 °C was improved by 4-fold in the presence of HP-β-CyD as proved by HPLC technique.

β-CyD was found to improve the solubility and dissolution profile of irbesartan [14]. By phase solubility diagram (PSD) analysis, the K_{11} value was found to be $1.04 \times 10^2\ M^{-1}$ in un-buffered water. The irbesartan/β-CyD solid systems were prepared by co-grinding, kneading, and co-evaporation. Among these methods, co-evaporation showed the highest solubility enhancement. The effect of water-soluble polymers (PEG 4000 or PVP K-90) as a third component on the complexation of irbesartan with β-CyD was investigated [15]. The study revealed that the binding and solubility were enhanced in the presence of the third component in comparison with the binary system of irbesartan and β-CyD.

Interaction of telmisartan with CyDs was studied by various techniques [16]. The results indicated that it forms 1:2 inclusion complexes with β-CyD and HP-β-CyD with complex formation constants of 0.7×10^3 and $2.4 \times 10^3\ M^{-1}$, respectively. The solid telmisartan/HP-β-CyD complexes were prepared by kneading and co-evaporation methods. The complex prepared with the kneading method showed the highest improvement in dissolution profile. In all studies [12–16], inclusion complexes formation in solution and solid state was proved by several techniques such as ^{13}C NMR, ^{1}H NMR, X-ray powder diffractometry (XRPD), differential scanning calorimetry (DSC), Fourier-transform infrared (FT-IR), and scanning electron microscopy (SEM).

The main objective of this work is to conduct a systematic study of the effect of CyDs on the solubility and stability of CAND. This investigation includes study the effect of: (1) different CyDs on the solubility of CAND by phase solubility diagram (PSD), (2) temperature on the solubility of CAND in the absence and presence of β-CyD, (3) method of preparation of CAND/β-CyD complex including kneading (KN), freeze drying (FD) and co-evaporation (EV) methods on the stability of CAND by HPLC technique, and (4) characterization of the solid complex by X-ray powder diffractometry (XRPD) and differential scanning calorimetry (DSC) techniques. In addition, Molecular mechanical modelling (MM) calculations will also be used to obtain theoretical information as to the most probable structure of the complex, and to explain the way that reaction may undergo and to determine the optimal structure and lowest energies may be taken through complexation.

2. Experimental

2.1. Materials

CAND (99.4%) from Ranbaxy Lab. Limited (India), α-CyD (99.3%), β-CyD (101.0%) and γ-CyD (98.7%) were produced by Wacker Chemie (Germany), hydroxypropyl-β-CyD (HP-β-CyD with a degree of substitution of 6.3 was produced by Yiming Fine Chemicals (China). All of the above materials were provided by The Jordanian Pharmaceutical Manufacturing Company (JPM). Other chemicals were of analytical grade obtained from Merck (Germany) and Across Organic (Belgium).

2.2. Instruments

UV/Visible spectrophotometer (Du-650i, Beckman, USA). HPLC instrument (Thermo Finnigan/USA) equipped with pump (P2000), detector (UV1000) and autosampler (AS3000). Thermostatic bath shaker (1086, GFL, Germany) connected to a chiller (23 DT 662-1, Heto-Holten, Denmark). pH-meter (3030, Jenway, England). Freeze dryer (FD3, Heto-Holten A/S, Denmark). Rotovapor (RV06-ML, IKA-WERKE, Germany) connected with pump (DOA-P504-BN, Gast/USA). Incubator (HC 0020, Heraeus/Germany). Manual hydraulic press (15000, Graseby Specac/USA). Halogen moisture analyzer (HR 73, Mettler/Switzerland). X-ray diffractometer (Philips PW 1729, Japan). Differential scanning calorimeter (910S, TA instrument, USA).

2.3. Phase solubility studies

Solubility studies were performed as described earlier [17]. Excess amounts of CAND (50 mg) were added to 50 ml of 0.1 M phosphate buffer solutions (pH = 8.0). Different amounts of CyDs were added to the buffer solution to obtain CyD concentrations ranging from 0 to 10 mM. The samples were shaken in a thermostat shaker at ~200 rpm to attain equilibrium (2 days) and then left overnight to settle at same temperature (16–40 °C), an aliquot was filtered using a 0.45 μm filter. The pH of the filtrate was measured by pH-meter. After a suitable dilution, the CAND content was determined spectrophotometrically by measuring the absorbances at λ_{max} of 256 nm. PSDs were analyzed to obtain estimates of the complex formation constants of soluble complexes following rigorous procedures described earlier [18,19]. Rigorous nonlinear regression of experimental data corresponding to each phase diagram was conducted to obtain estimates of complex formation constants (K_{ij}).

2.4. Complex preparations

2.4.1. Kneading method (KN)

CAND (4 g) and β-CyD (8 g) were well mixed together in a mortar and then water (4 ml) was added (in portions) so as to obtain a homogeneous paste. The mixture was then ground for 30 min. During this process, an appropriate quantity of water was added to the mixture in order to maintain a suitable consistency. The paste was dried in oven at 40 °C for 24 h. The dried complex was pulverized into a fine powder.

2.4.2. Freeze-drying method (FD)

CAND (0.2 g) and β-CyD (0.4 g) were separately dissolved in 10 ml and 20 ml of ethanol and water, respectively. The solutions thus obtained were mixed and freeze-dried for 1 day and the solids were collected.

2.4.3. Co-evaporation method (EV)

CAND (1 g) and β-CyD (2 g) were separately dissolved in 50 ml and 100 ml of ethanol and water, respectively. The solution thus

obtained was evaporated at 60 °C to dryness and the solid was collected.

2.4.4. Physical mixture preparation (PM)

Physical mixtures of CAND and β-CyD in the same molar ratio pertaining to complex stoichiometry were prepared by mixing of pulverized powder of each component, which was previously treated separately as in complex preparations.

2.5. Characterization of CAND/β-CyD complex

2.5.1. X-ray powder diffractometry (XRPD)

The XRPD patterns were measured with X-ray diffractometer. Radiations generated from Co K_α source and filtered through Ni filters with a wavelength of 1.79025 Å at 40 mA and 35 kV were used. The instrument was operated with a scanning rate of 0.02° s^{-1} over the 2θ range of 5–55°.

2.5.2. Differential scanning calorimetry (DSC)

The thermal behaviour of all samples of CAND, β-CyD, a physical mixture of CAND and β-CyD, and the isolated CAND/β-CyD solid complex were studied by DSC. Accurately weighed sample of each equivalent to 5 mg CAND was heated in a sealed aluminum pan, using an empty pan sealed as reference, over the temperature range of 30 to 300 °C, at a rate of 10 °C/min. Indium standard was used for calibrating the temperature.

2.6. Stability study

2.6.1. Sample preparation

The complexes prepared by different methods (KN, FD and EV), CAND and their corresponding PMs were incubated at room temperature (25 °C) and at 40 °C/75% relative humidity for different periods of time. Samples (each equivalent to 30 mg CAND) at each interval were separately transferred to 100 ml volumetric flasks, acetonitrile (70 ml) was added and the samples were shaken for 15 min. Then the volume was completed to 100 ml with acetonitrile and mixed. Portions of the solutions were filtered and then 20 μl were injected on the HPLC to measure the content of CAND.

2.6.2. High performance liquid chromatography (HPLC)

The HPLC system was equipped with a 254 nm detector and 250 mm × 4.6 mm column that contained 5 μm packing L1 (Hypersil ODS, 250 mm × 4.6 mm is suitable). The system was operated at ambient temperature. The mobile phase composed of 0.02 M potassium dihydrogen phosphate solution and acetonitrile (2:8, v/v). The pH of the mixture was adjusted to pH 4.0 with 85% phosphoric acid. The flow rate was about 1 ml/min. The HPLC method was developed and validated to be used as stability indicating method. Different parameters were manipulated to obtain an acceptable resolution between the analyte components with acceptable recoveries and to satisfy the HPLC system suitability. These parameters included: mobile phase composition and its pH, flow rate, column temperature, and different types of columns. In addition, all validation parameters including specificity, repeatability, linearity and range, robustness, limit of detection and limit of quantitation were considered.

2.7. Molecular mechanical modelling (MM)

MM was performed in vacuum and water using Hyperchem® (release 8.06). Force fields used in these computations were Amber and enhanced MM method implemented in Hyperchem using the atomic charges or bond dipoles options for calculation of electrostatic interactions. Bond, angle, torsion, non-bonded, electrostatic and hydrogen-bonded interactions were calculated in both MM^+ and amber force fields. Partial atomic charges were obtained by performing AM1 semi-empirical calculations and the value of charge on each atom (total number of CAND atoms is 80) was assigned.

Energy minimizations were obtained using the conjugate gradient algorithm (0.1 kcal/mol Å) gradient. The starting geometries of CyDs were obtained using X-ray diffraction data. These geometries were optimized again using the Amber force field by imposing a restraint on the dihedral angles to the average values. CAND was built up from natural bond angles, as defined in this software, the structures were then minimized with the MM and Amber force field, the resulting structure was further optimized at the HF-ab initio level with the 3-21G* basis set.

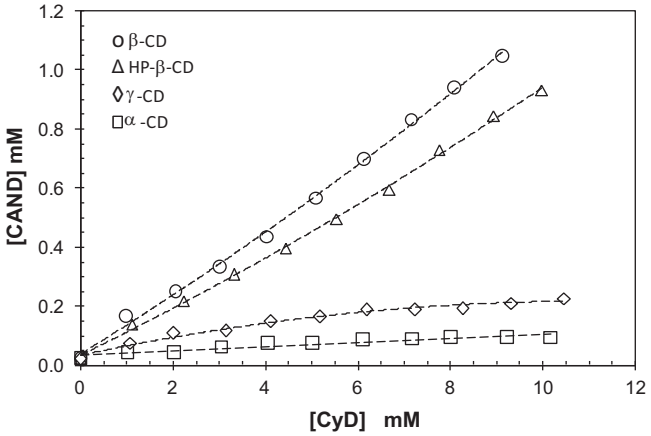

Fig. 2. Phase solubility diagrams of the CAND/CyD systems in 0.1 M phosphate buffer (pH 8.0) at 25 °C.

3. Results and discussion

3.1. Interaction of candesartan cilexetil with CyDs in solution

3.1.1. Effect of CyD type

Fig. 2 depicts phase solubility diagrams (PSDs) obtained for CAND against each of α-, β-, HP-β- and γ-CyD concentration in 0.1 M phosphate buffers (pH = 8.0) and 25 °C. At this pH, CAND (pK_a = 6.0) has an inherent solubility (S_o) of 2.13×10^{-2} mM [7]. Rigorous nonlinear regression of experimental data corresponding to each phase diagram was conducted [18,19] to obtain estimates of complex formation constants (K_{ij}). The results indicated the formation of 1:1 and 1:2 CAND/CyD complexes with β- and HP-β-CyDs. The K_{12} obtained by rigorous analysis was relatively lower than K_{11}, so K_{11} was used as an index to study the effect of various factors on complex stability as discussed below.

The K_{11} values were 5.87×10^3, 4.49×10^3, 0.94×10^3 and 0.40×10^3 M^{-1} for β-CyD, HP-β-CyD, γ-CyD and α-CyD, respectively (Table 1). The low K_{11} values in case of α-CyD and γ-CyD are most likely due to two factors: (a) they are highly soluble in water thus lowering the driving force to complex with CAND, and (b) α-CyD has a small cavity size that reduces the probability of including the bulky groups of CAND, while γ-CyD has a large cavity size thus

Table 1
Estimates of complex formation constants (K_{11} and K_{12}) for the CAND/CyD systems in 0.1 M phosphate buffer at pH 8.0 and 25 °C.

CyD	Phase solubility diagram type	$K_{11} \times 10^{-3}$ (M^{-1})	$K_{12} \times 10^{-3}$ (M^{-1})
β-CyD	A_L	5.87	0.019
HP-β-CyD	A_L	4.49	0.020
γ-CyD	A_L	0.94	0.0
α-CyD	A_L	0.40	0.0

Table 2
Estimates of complex formation constants (K_{11}) of the CAND/β-CyD system obtained in 0.1 M phosphate buffer (pH 8.0) and different temperatures, and the thermodynamic parameters corresponding to K_{11} and CAND solubility (S_o) obtained from van't Hoff plots.

T (°C)	$S_o \times 10^2$ (mM)	$K_{11} \times 10^{-3}$ (M^{-1})
16.1	1.25	9.19
20.4	1.79	6.60
25.4	2.13	5.87
29.3	2.95	4.69
35.1	3.74	3.84

	ΔG° (kJ/mol)	ΔH° (kJ/mol)	ΔS° (J/mol K)
CAND/β-CyD complex	−31.5	−32.8	−4.6
Solubility of CAND (S_o)	36.5	42.2	18.9

lowering effective interactions with CAND [20,21]. The lower binding of CAND with HP-β-CyD compared to β-CyD is probably due to the presence of substituent hydroxypropyl groups at the rims of the-β-CyD cavity in HP-β-CyD, which may retard the inclusion of CAND via steric hindrance [20]. Although the HP-β-CyD has high aqueous solubility similar to α-CyD and γ-CyD, it shows higher binding constant ($4.49 \times 10^3\ M^{-1}$) in comparison with the obtained values of α-CyD ($0.40 \times 10^3\ M^{-1}$) and γ-CyD ($0.94 \times 10^3\ M^{-1}$). This most probably indicates that the cavity size of CyDs plays an important role in complex formation and their binding strength.

It is worth mentioning that in the previous works on various sartan members [12–16], the empirical equation $K_{11} = \text{slope}/S_o(1 - \text{slope})$ was used to find the K_{11} values rather than using nonlinear regression analysis [18,19]. This may lead to failure in prediction the formation of higher order complexes (SL_n, where $n = 2, 3, \ldots$) with the CyD. In addition, the PSDs were constructed in un-buffered water, which may make it difficult to compare the reported results with the present finding in this work. Generally, CAND and telmisartan showed strong binding with β-CyD and HP-β-CyD (magnitude of 10^3) comparing with valsartan and irbesartan (magnitude of 10^2). This indicates that the geometrical structure and type of substituent (e.g. hydrophobic or hydrophilic character) have influence on the extent of binding of the guest with CyD.

Due to the fact that complex of CAND with β-CyD has relatively high K_{11} values compared with the other CyDs (Table 1), it was chosen for the further investigation, as shown below, to evaluate the driving forces for complex formation (by thermodynamic), to verify inclusion complex formation (by DSC), to test the chemical stability of CAND in the presence of β-CyD (by HPLC), and to explore guest–host interaction sites (by MM).

3.1.2. Thermodynamics

The PSDs of CAND obtained in 0.1 M phosphate buffer (pH 8.0) at different temperatures are shown in Fig. 3A. The corresponding complex formation constants (K_{11}) and the solubilities of CAND in the absence of β-CyD (S_o) are listed in Table 2. van't Hoff plots of $\ln K_{11}^x$ and $\ln S_o^x$ against $1/T$ are shown in Fig. 3B, while the thermodynamic parameters (ΔH°, ΔS° and ΔG°) are listed in Table 2.

The results suggest that CAND/β-CyD complex formation ($\Delta G^\circ = -31.5$ kJ/mol) is largely driven by enthalpy ($\Delta H^\circ = -32.8$ kJ/mol), which is attributed to van der Waals interactions, H-bonding between the guest and host, or due to loss of water upon complexation. The corresponding negative entropy change ($\Delta S^\circ = -4.6$ J/mol K), is attributed to a reduction of the translational and rotational degrees of freedom of the guest molecule rather than to solvent disordering [22]. CAND solubility ($\Delta G^\circ = 36.5$ kJ/mol) is impeded by enthalpy ($\Delta H^\circ = 42.2$ kJ/mol). The positive enthalpy indicates that energy is needed to break a molecule away from its pure phase and to separate the water molecules so there is a vacant space or "cavity" for the incoming molecule, while the solubility is favoured by entropy changes ($\Delta S^\circ = 18.9$ J/mol K) leading to a more random structure (i.e. $+\Delta S$) [23].

3.2. Characterization of CAND/β-CyD solid complex

Fig. 4 shows the thermal behaviours of all samples of CAND, a physical mixture of 1:1 CAND and β-CyD, and the isolated 1:1 CAND/β-CyD solid complexes. The DSC thermogram of kneaded CAND (Fig. 4A) showed a sharp endothermic peak at about 167 °C. This peak is retained in both the complex prepared by KN method and physical mixture (prepared by mixing kneaded CAND and kneaded β-CyD) indicating that KN method does not produce real inclusion complex. In contrast, the DSC thermograms of freeze-dried CAND, the physical mixture and complex prepared by FD method (Fig. 4B) showed the complete disappearance of the CAND endothermic peak, which suggests the formation of a real inclusion complex and/or amorphous phase [24–26]. In the case of complex prepared by EV method, the real complex is proved by the disappearance of the endothermic peak of CAND (Fig. 4C), which is retained in the DSC thermograms of evaporated CAND and its physical mixture with β-CyD.

3.3. Effect of β-CyD on the stability of candesartan cilexetil in solid state

CAND was found stable at ambient conditions for 3 years. It was stable as well when stored in open containers at 40 °C/75% rela-

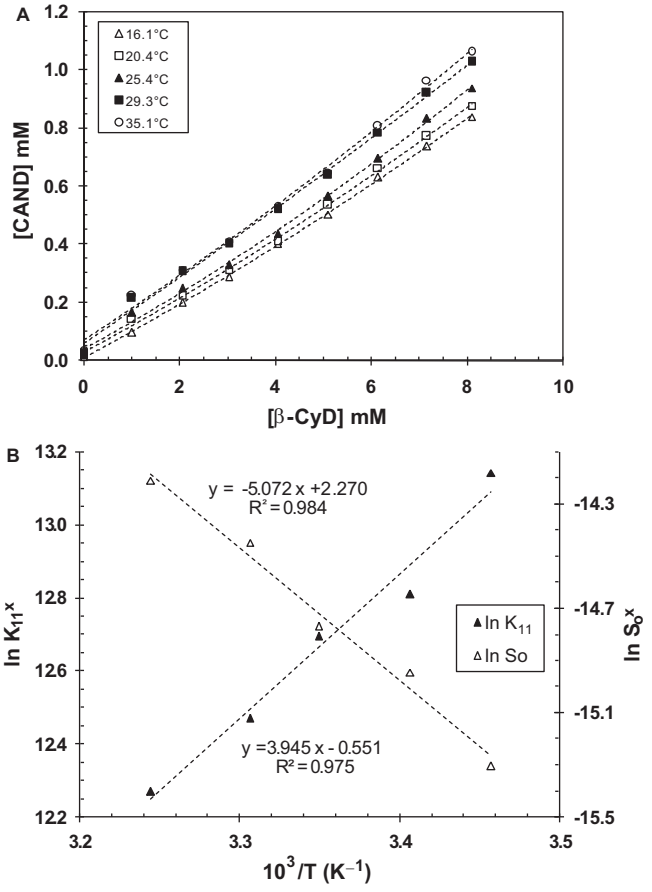

Fig. 3. (A) Phase solubility diagrams of the CAND/β-CyD system in 0.1 M phosphate buffer (pH 8.0) at different temperatures and (B) plots of $\ln K_{11}^x$ and $\ln S_o^x$ against $1/T$ (x denotes the mole fraction standard state).

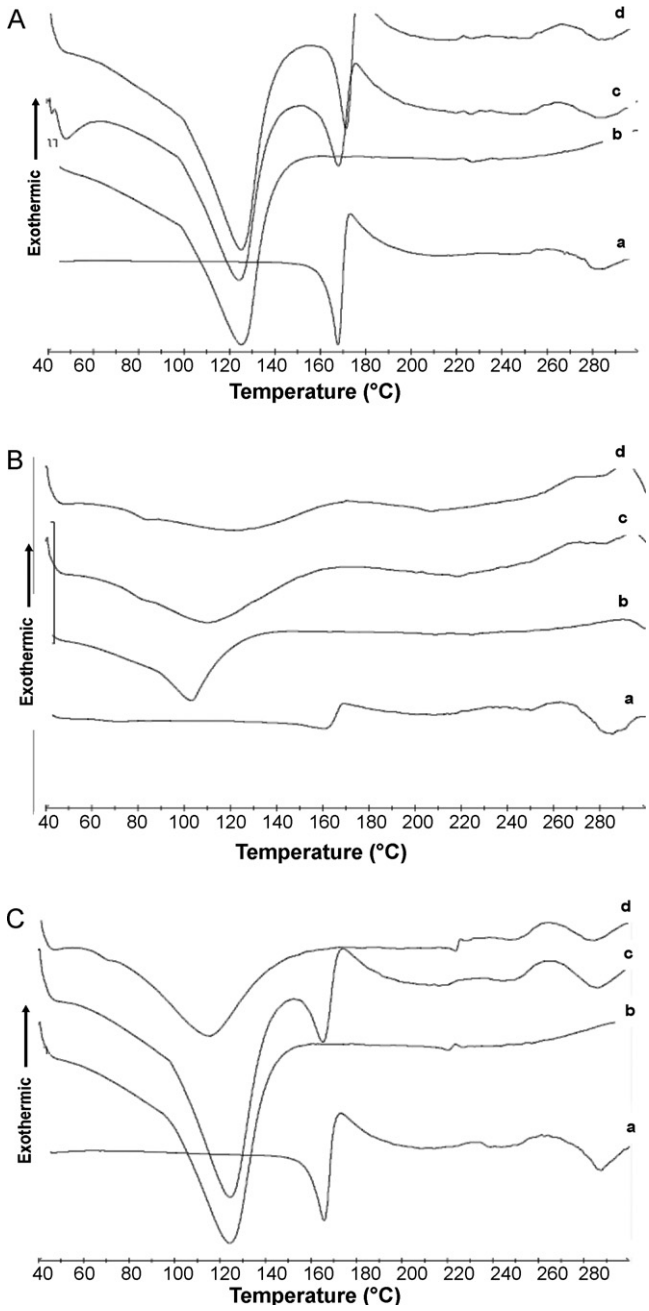

Fig. 4. DSC thermograms of CAND/β-CyD system: (A) kneading, (B) freeze drying and (C) co-evaporation methods, where (a) CAND, (b) β-CyD, (c) a physical mixture of 1:1 CAND and β-CyD, and (d) 1:1 CAND/β-CyD complex.

tive humidity and 50 °C/75% relative humidity for 3 months and 1 month, respectively, where it showed no loss in potency and absence of any degradation products. Exposure to sunlight and UV light for 1 month similarly showed no loss in potency and absence of any degradation product.

Although CAND is stable against temperature, moisture and light when it is alone in the solid state, but when it is formulated into tablets with other ingredients, decomposition can be observed with the lapse of time due to deformation of crystals caused by, for example, pressure, abrasion and heat, applied in the step of granulation or molding under elevated pressure in the course of preparation, because of that an elastic material should be involved to overcome this problem [8].

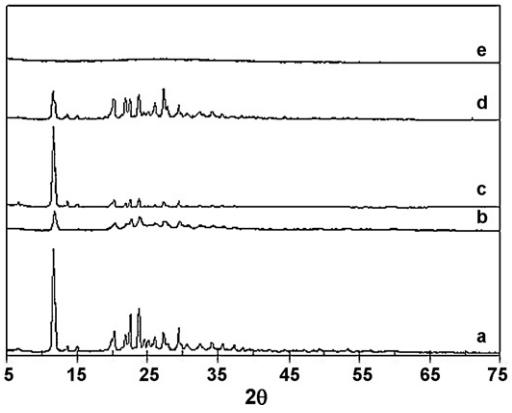

Fig. 5. XRPD patterns of CAND before (a) and after (b) compression, (c) kneading, (d) evaporation and (e) freeze drying.

In this work, the stability of complexes prepared by KN, EV and FD methods was monitored by HPLC method and all the stability results obtained are listed in Table 3. The results indicated that the degree of degradation with respect to the method used to prepare the complex follows the order: FD > EV > KN. It is clear that amorphous CAND in its pure state or as complex with β-CyD is instable comparing with the crystalline form. The investigation of solid phase transformation of CAND by DSC (Fig. 4B) and XRPD (Fig. 5) techniques proved such assumption. Also it is worth mentioning that when CAND is compressed in disk it losses partially its crystallinity as detected by XRPD (Fig. 5). Also the results indicated that, in case of KN and EV methods, when the sample kept as powder is more stable than compressed one in disk (Table 3), which is most probable due to enhancing the interaction and loss of CAND crystallinity (e.g. formation of amorphous) with compression [8]. This may suggest formulating CAND into powder filled in capsule

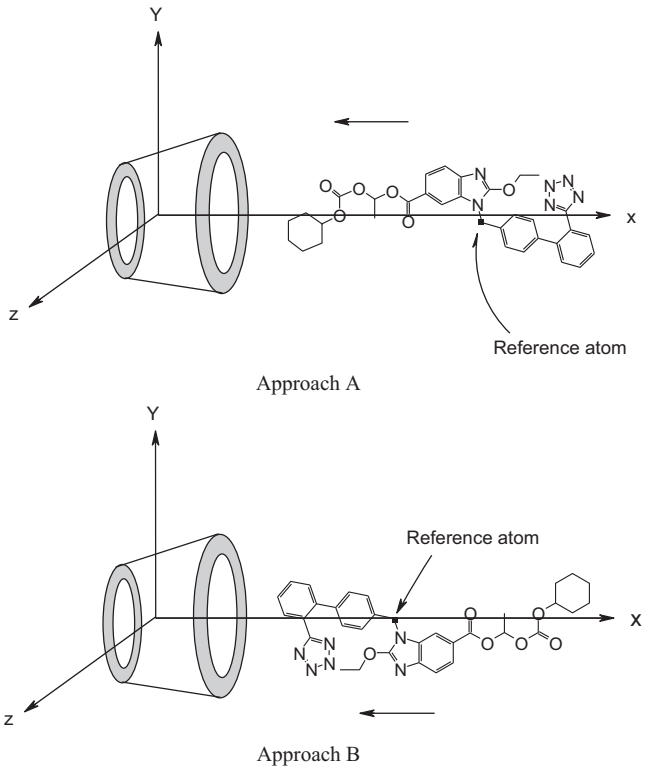

Fig. 6. Coordinate systems for the 1:1 CAND complexation process with β-CyD by A and B guest–host approaches.

Table 3
The Stability data of CAND/β-CyD systems at 40 °C/75% relative humidity.

Sample	Initial			6 month		
	CAND	Maximum degradant	Total degradants	CAND	Maximum degradant	Total degradants
Freeze drying (%)						
CAND (powder)	99.2	0.3	0.9	99.2	0.3	0.9
CAND (Disk)	99.2	0.3	0.9	99.2	0.3	0.9
Freeze-dried CAND (powder)	95.8	1.5	4.2	44.2	10.0	55.8
Freeze-dried CAND (disk)	95.8	1.5	4.2	45.4	16.5	54.6
Phys. mix. (powder)	95.5	1.9	4.5	45.0	12.0	55.0
Phys. mix. (disk)	95.5	1.9	4.5	38.2	18.7	61.8
Complex (powder)	94.7	1.8	5.4	56.1	36.8	43.9
Complex (disk)	94.7	1.8	5.4	65.6	20.3	34.4
Co-evaporation (%)						
Evaporated CAND (powder)	99.3	0.4	0.7	99.2	0.4	0.8
Evaporated CAND (disk)	99.2	0.3	0.9	96.8	1.2	3.2
Phys. mix. (powder)	99.0	0.4	1.0	99.0	0.4	1.1
Phys. mix (disk)	99.0	0.4	1.0	95.3	1.7	4.7
Complex (powder)	99.0	0.4	1.1	99.0	0.4	1.2
Complex (disk)	96.2	1.7	3.8	92.2	2.8	7.7
Kneading (%)						
Kneaded CAND (powder)	99.1	0.4	1.0	99.1	0.4	0.9
Kneaded CAND (disk)	99.1	0.4	1.0	97.0	0.9	3.0
Phys. mix. (powder)	99.1	0.4	0.9	99.1	0.4	0.9
Phys. mix. (Disk)	99.0	0.4	1.0	96.8	0.9	3.2
Complex (powder)	99.2	0.4	0.8	99.1	0.4	0.9
Complex (disk)	99.0	0.4	1.1	95.8	1.5	4.2

Maximum degradant is desethyl CAND.

rather than compressed in tablet dosage form. As a result, formulating CAND in the presence of β-CyD by KN and EV methods may enhance the solubility of CAND with acceptable stability.

3.4. Molecular mechanical modelling (MM) and optimal complex configurations

The tertiary inertial axis of β-CyD was set at the *x*-axis, and the secondary inertial axis was set at the *y*-axis. The center of mass of the ether oxygens in the β-CyD was located at the origin of the Cartesians coordinate, while that of the CAND molecule was set at an atom close to its center of mass. Initially, the position of the β-CyD macrocyclic was fixed while the guest approaches along the *x*-axis toward the wider rim of the β-CyD cavity. The coordinate system used to define the process of complexation is shown below for the two approaches A and B (Fig. 6).

Starting at −20 Å, the energy of the guest was minimized all the way through +20 Å from the origin of the Cartesian coordinate, which was designated by the center of the ether glycosidic oxygens of β-CyD and an atom close the center of mass of the guest molecule

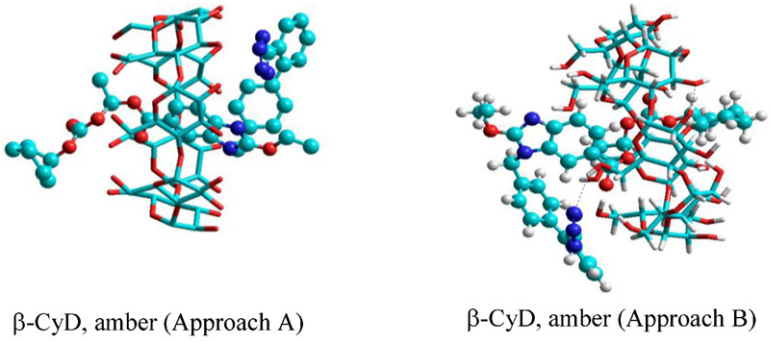

Fig. 7. Side views of the most probable CAND/β-CyD configurations obtained for the 1:1 complex through approaches A and B using different force fields.

at 2 Å intervals. The structure generated at each step was optimized from the initial conformations, while keeping the β-CyD structure fixed. At the energy minimum thus obtained, the whole system was allowed to interact free of restrictions using a 0.10 kcal/mol Å gradient to obtain the optimal host–guest complex (SL complex) geometry.

The non-bonded interactions energy between CAND and β-CyD, or binding energy, $E_{binding}$ was estimated according to the relation

$$E_{binding} = E_{CAND/CD\,Complex} - (E_{isolated\,CAND} + E_{isolated\,CD})$$

where the terms on the right hand side, represent the potential energy of the CAND/β-CyD system minus the sum of the potential energies of isolated CAND and isolated β-CyD in the same conformation.

The binding energy ($E_{binding}$) was plotted against the *x*-coordinate for approaches A and B using $MM_{bond\ dipoles}$, $MM_{atomic\ charges}$, and Amber force fields. The results showed that Amber force field gave the most stable geometry for CAND/β-CyD (−167.4 and −179.9 kJ/mol for approaches A and B, respectively). MM atomic charge and MM bond dipoles have less binding energy (−146 kJ/mol for both).

The fact that the three force fields predict different $E_{binding}$ values, for the same system and same approach, is due to the use of different model compounds in the parameterization procedures of these force fields [27,28]. Accordingly, $E_{binding}$ values can be used to indicate which complex geometry is more favourable but no more quantitative significance can be attached to the absolute values, especially when comparing $E_{binding}$ values obtained from different force fields [27].

Fig. 7 depicts side views of the optimal 1:1 complex configurations obtained for CAND with β-CyD. In all complexes, CAND penetrated the cavity completely. The most stable β-CyD inclusion complexes (approach B) reveal one hydrogen bond between β-CyD primary hydroxyls and the nitrogen atom in tetrazole moiety of CAND (Fig. 7), where nitrogen atom in tetrazole moiety has the highest negative charge value (−0.19), which facilitates the interaction with β-CyD primary hydroxyls.

4. Conclusion

The results of this study on CAND/CyDs complexation in aqueous solution reveal that the tendency of CAND ($pK_a = 6.0$) to complex with CyDs follows the order: β-CyD > HP-β-CyD > γ-CyD > α-CyD indicating that size fit and steric hindrance play an important role in complex formation. Complex formation of CAND with β-CyD ($\Delta G^\circ = -31.5$ kJ/mol) is largely driven by enthalpy change ($\Delta H^\circ = -32.8$ kJ/mol), which is attributed to van der Waals interactions, H-bonding between the guest and host, or due to loss of water upon complexation. The corresponding negative entropy change ($\Delta S^\circ = -4.6$ J/mol K), is attributed to a reduction of the translational and rotational degrees of freedom of the guest molecule rather than to solvent disordering. The stability results suggested formulating CAND with β-CyD by kneading or evaporation methods into capsule dosage form rather than freeze drying, which forms less stable amorphous CAND. DSC and MM simulation of possible CAND/β-CyD interaction provides inside view on CAND/β-CyD interaction mechanisms prevailing in aqueous solutions with penetration of CAND molecule inside the cavity of β-CyD.

Acknowledgment

We wish to thank faculty of graduate studies at Al al-Bayt University for financial support.

References

[1] V.J. Stella, R.A. Rajewski, Cyclodextrins: their future in drug formulation and delivery, Pharm. Res. 14 (1997) 556–567.
[2] D. Duchene, Cyclodextrins and Their Industrial Uses, Editions de Sante', Paris (France), 1987.
[3] T. Loftsson, D. Duchene, Cyclodextrins and their therapeutic applications, Int. J. Pharm. 329 (2007) 1–11.
[4] E.M.M. Del Valle, Cyclodextrins and their uses: a review, Process Biochem. 39 (2004) 1033–1046.
[5] N. Ferreirós, S. Dresen, R.M. Alonso, W. Weinmann, Hydrolysis and transesterification reactions of candesartan cilexetil observed during the solid phase extraction procedure, J. Chromatogr. B. 855 (2007) 134–138.
[6] ATACAND® product monograph, http://www.astrazeneca.ca/documents/ProductPortfolio/ATACAND_PM_en.pdf (accessed 19.05.10).
[7] E. Cagigal, L. González, R.M. Alonso, R.M. Jiménez, p*Ka* determination of angiotensin II receptor antagonistic (ARA II) by spectrofluorimetry, J. Pharm. Biomed. Anal. 26 (2001) 477–486.
[8] M. Tadashi, Pharmaceutical Compositions with Angiotensin-II-Antagonistic activity, Patent No. 0546358. Application No. 92119705.9, 1993.
[9] S. Helene, L. Per-Olof, C. Andersen, Determination of candesartan cilexetil, candesartan and a metabolite in human plasma and urine by liquid chromatography and fluorometric detection, J. Chromatogr. B 731 (1999) 411–417.
[10] D.V. Subba Rao, P. Radhakrishnanand, M.V. Suryanarayana, V. Himabindu, A stability-indicating LC method for candesartan cilexetil, Chromatographia 66 (2007) 499–507.
[11] A. Mohan, S. Shanmugavel, A. Goyal, B.R. Venkataraman, D. Saravanan, Identification, isolation, and characterization of five potential degradation impurities in candesartan cilexetil tablets, Chromatographia 69 (2009) 1–10.
[12] B Cappello, C. Di Maio, M. Iervolino, A. Miro, Improvement of solubility and stability of valsartan by hydroxypropyl-β-cyclodextrin, J. Incl. Phenom. Macrocyclic Chem. 54 (2006) 289–294.
[13] N. Pravin, A. Babasaheb, D. Neha, K. Vilasrao, H. Rajashree, Solis state characterization of the inclusion complex of valsartan with methyl β-cyclodextrin, J. Incl. Phenom. Macrocyclic Chem. 65 (2009) 377–383.
[14] H. Rajashree, K. Vilasrao, Preformulation study of the inclusion complex of irbesartan–β-cyclodextrin, AAPS PharmSciTech 10 (2009) 276–281.
[15] S.H. Rajashree, N.S. Suneeta, J.K. Vilasrao, Studies on the effect of water-soluble polymers on drug–β-cyclodextrin complex solubility, AAPS PharmSciTech 10 (2009) 858–863.
[16] N.K. Rajesh, S.K. Bhanudas, Preparation, physicochemical characterization, dissolution and formulation studies of telmisartan cyclodextrin inclusion complexes, Asian J. Pharm. 4 (2010) 52–59.
[17] T Higuchi, K.A. Connors, Phase solubility techniques, Adv. Anal. Chem. Instrum. 4 (1965) 117–212.
[18] M.B. Zughul, A.A. Badwan, SL_2 type phase solubility diagrams, complex formation and chemical speciation of soluble species, J. Incl. Phenom. Macrocyclic Chem. 31 (1998) 243–264.
[19] M.B. Zughul, Rigorous nonlinear regression analysis of phase solubility diagrams to obtain complex stoichiometry and true thermodynamic drug–cyclodextrin complexation parameters, J. Incl. Phenom. Macrocyclic Chem. 57 (2007) 525.
[20] L. Ribeiro, F. Veiga, Complexation of vinpocetine with cyclodextrins in the presence or absence of polymers, binary and ternary complexes preparation and characterization, J. Incl. Phenom. Macrocyclic Chem. 44 (2002) 251–256.
[21] J. Taraszewska, K. Migut, M. Kozbiat, Complexation of flutamide by native and modified cyclodextrins, J. Phys. Org. Chem. 16 (2003) 121–126.
[22] L.L. Yannis, V. Varka, G. Gregoriadis, Novel non-acidic formulations of haloperidol complexed with β-cyclodextrin derivatives, J. Pharm. Biomed. Anal. 16 (1997) 263–268.
[23] R.E. Saichek, K.R. Reddy, Electrokinetically enhanced remediation of hydrophobic organic compounds in soils, Crit. Rev. Environ. Sci. Technol. 35 (2005) 115–192.
[24] E. Redenti, T. Peveri, M. Zanol, P. Ventura, G. Gnappi, A. Montenero, A study on the differentiation between amorphous piroxicam–β-cyclodextrin complex and a mixture of the two amorphous components, Int. J. Pharm. 129 (1996) 289–294.
[25] H. Matsunaga, T. Eguchi, K. Nishijima, T. Enomoto, K. Sasaoki, N. Nakamura, Solid-state characterization of candesartan cilexetil (TCV-116): crystal structure and molecular mobility, Chem. Pharm. Bull. 47 (1999) 182–186.
[26] M. Cirri, F. Maestrelli, N. Mennini, P. Mura, Physical–chemical characterization of binary and ternary systems of ketoprofen with cyclodextrins and phospholipids, J. Pharm. Biomed. Anal. 50 (2009) 683–689.
[27] N.L. Allinger, Y.H. Yuh, J.H. Lii, Molecular mechanics (MM3) force field for hydrocarbons, J. Am. Chem. Soc. 111 (1989) 8551–8558.
[28] W.D. Cornel, P. Cieplak, C.L. Bayly, I.R. Gould, K.M. Mertz, D.M. Ferguston, D.C. Spellmeyer, T. Fox, J.W. Caldwell, P.A. Kollman, A second generation force field for the simulation of proteins, nucleic acids, and organic molecules, J. Am. Chem. Soc. 117 (1995) 5179–5197.